Supporting Information

Quantitative measurements of protein volume and concentration using hydrogel-backed nanopores

*Reyhaneh Nazarian, Eric Lee, Brian Siegel, Chance Kuo, Shiv Acharya, Jacob Schmidt**

UCLA Department of Bioengineering, 420 Westwood Plaza, Los Angeles, CA 90095

S1- Materials and methods

Apparatus Diagram:

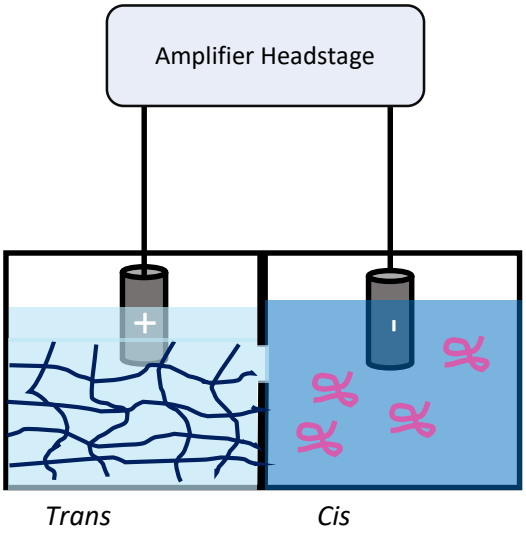

Figure S1. Schematic diagram of measurement apparatus. The nanopore chip separates the hydrogel-containing *trans* chamber from the protein containing *cis* chamber. In this work, pH 10 buffer was used and all proteins were negatively charged. A negative applied voltage (*cis* electrode – *trans* electrode) drives the proteins into the nanopore for detection by the amplifier.

Materials: All chemicals were purchased from Sigma-Aldrich at reagent grade and used as received. Immunoglobulin gamma (IgG), ovalbumin, and poly-L-glutamic acid sodium were purchased from Sigma-Aldrich. Purified myoglobin was generously provided by the Steven Jacobsen lab at UCLA. IgG, ovalbumin, and myoglobin were chosen as the common protein standards for biological studies.

Nanopore fabrication and hydrogel polymerization: 15 nm thick silicon nitride membranes were commercially purchased from Ted Pella Inc.; membranes were PDMS coated and cured for several hours at 120°C before use. Silicon nitride membranes were plasma treated for 30 sec, mounted in a Teflon fluidic cell, and degassed. Nanopores were formed using dielectric breakdown in 2 M KCl, pH 10 at the desired size as previously reported.[1] PEG-DMA hydrogel solution was prepared by mixing 10% (w/v) PEG-1000 Dimethylacrylamide in 2 M KCl, 100 mM Tris-HCl at pH 10 (adjusted by HCl and NaOH), 10% (w/v) ammonium persulfide (APS), and 20% (w/v)

tetramethylethylenediamine (TEMED). Nanopore diameters were determined immediately after formation as described previously.[2] After formation of a nanopore, electrolyte in the compartment on the TEM window side was replaced with PEG-DMA hydrogel solution, and polymerized in-situ for 10 minutes before nanopore measurement.

Nanopore measurements: All nanopore measurements were carried out using an Axopatch 200B amplifier and Digidata 1440B or 1322A data acquisition at 100 kHz with a 10 kHz hardware low pass filter. Nanopore measurements were performed in 2 M KCl, 100 mM Tris-HCl, pH 8-10. At least 5 minutes of control measurements were run before protein injection. In all experiments, the hydrogel side (*trans*) of the nanopore chip was grounded, and protein was injected into the other side (*cis*) to make a final concentration of 1 fM – 2 µM; the *cis* solution was briefly stirred before measurements began with -50 to -100 mV applied (V_{cis}-V_{trans}).

Data analysis: All captured data were analyzed using a MATLAB script as previously reported.[1]

S2- Protein translocation rate following protein addition versus time

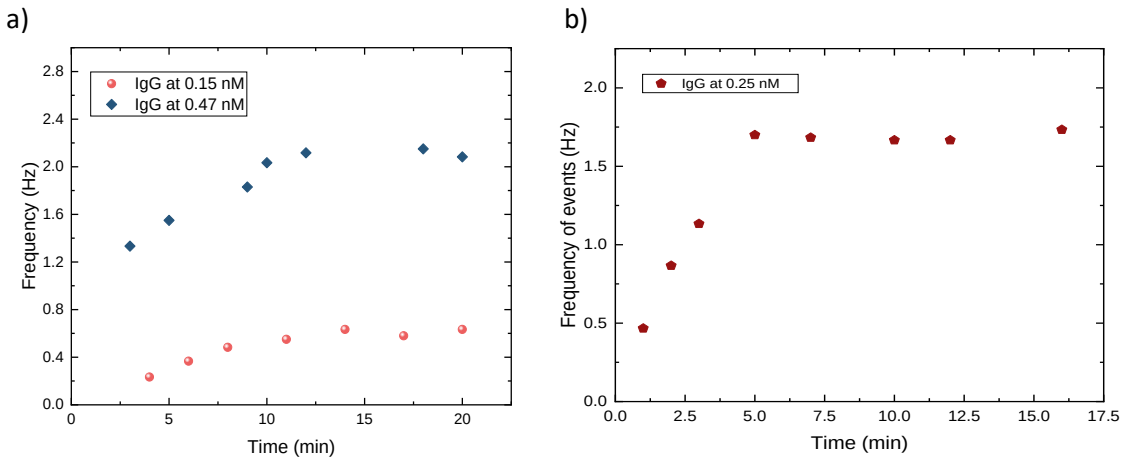

Figure S2. a) Measured event frequencies versus time of IgG at 0.15 and 0.47 nM after injection into the flow cell; 21 nm diameter nanopore. b) Measured event frequency of 0.25 nM IgG vs. time; 24 nm diameter nanopore. Data from both panels obtained with -50 mV applied potential.

S3- Observed event frequency versus protein concentration

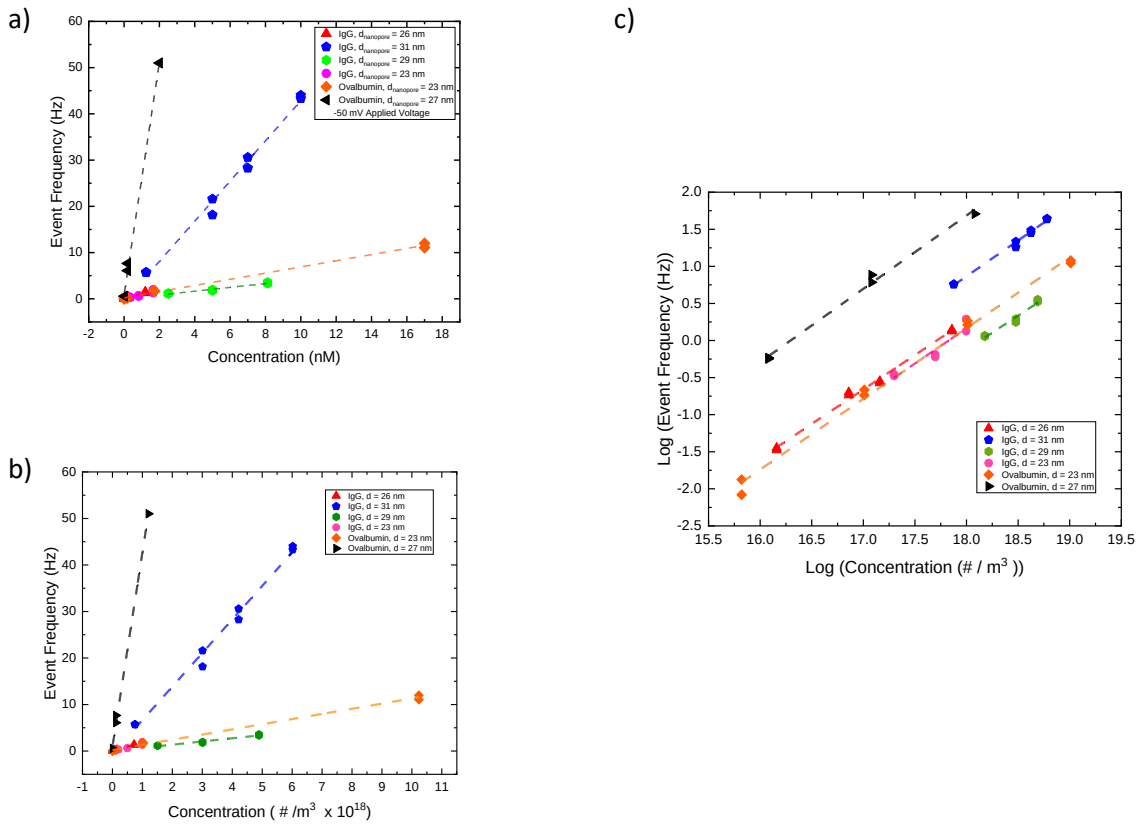

Figure S3. Linear relation of event frequency vs. protein bulk concentration. a) Event frequency (Hz) vs. concentration (nM); b) event frequency (Hz) vs. concentration (# / m^3 x 10^{18}); c) log (event frequency (Hz)) vs. log (concentration (# / m^3))

S4- Interpolation of unknown concentration using calibration data

Using the R computing environment (R-3.3.0), best-fit linear estimates of a calibration curve were obtained for each used nanopore based on 2 or 3 earlier observed data points. *Predict.lm* function was used to determine the unknown concentration of the last data point for each nanopore measurement based on the observed frequency, and also to determine the prediction confidence interval.

Table S1. Determination of unknown protein concentrations using hydrogel-backed nanopores

Nanopore Diam. (nm)	**Protein**	**# of Cal. Pts**	**Concentration (nM)**		**Confidence Interval**		**Error**
			Actual	Predicted	Lower (nM)	Upper (nM)	
29	IgG	2	8.12	11.22	5.88	21.37	38%
23	IgG	2	1.64	2.15	1.34	4.36	31%
27	Ovalbumin	2	2.00	1.28	0.58	2.75	36%
26	IgG	3	1.20	1.12	0.57	2.29	7%
31	IgG	3	10.00	10.71	8.05	14.12	7%
23	Ovalbumin	3	17.00	15.48	5.37	25.70	9%

S5- Predicted capture rate for a cylindrical nanopore based on generalized Smoluchowski equation:[3]

For a nanopore system with total applied voltage ΔV and potential drop from the access resistance of the nanopore δV, the potential at distance r from the opening of a nanopore with diameter d is given by:[3]

$$V(r) = \frac{d}{2r}\delta V \qquad \text{S1}$$

δV is difference of the total voltage drop ΔV and the voltage drop across the nanopore itself ($R_{nanopore}I_{nanopore}$), and is expressed as:

$$\delta V = \Delta V \frac{d/_{4l}}{1 + d/_{2l}} \qquad \text{S2}$$

where l is the nanopore length.

Substituting Equation S1 into S2 gives the voltage potential V(r) at distance r from a nanopore mouth in terms of the total applied voltage:

$$V(r) = \frac{d}{2r}\Delta V \frac{d/_{4l}}{1 + d/_{2l}} \qquad \text{S3}$$

For long and narrow nanopores (l >> d), Equation S3 is simplified to $V(r) = \frac{d^2}{8lr}\Delta V$.

In dilute solutions, particle interactions may be neglected, and the captured flux J is linearly proportional to the particle concentration c:

$$J = R_c c \qquad \text{S4}$$

where R_c is the capture rate per unit concentration.

To find the capture rate, Grosberg and Rabin assume a hemispherical capture zone at the nanopore entrance where the protein motion transitions from non-biased diffusion to electrophoretic drift. They assume that all proteins enter the capture zone are driven into the nanopore to be detected. Further they assume that the particles are driven to the mouth of the nanopore by the net sum of the gradients in concentration and the electric potential. Thus, the particle flux j is:

$$j = -D\,\nabla c + \mu c \nabla V \qquad \text{S5}$$

where D and μ are the particle's diffusion constant and the electrophoretic mobility.

Solving the continuity equation ($\frac{\partial c}{\partial t} + \nabla . j = 0$) with a Coulomb potential ($V(r) = \frac{q_{eff}}{\varepsilon r}$) with boundary conditions of

$$c(\infty) = c$$
$$c\,(r_0) = 0 \qquad \text{S6}$$

(where r_0 is the distance from the pore where particles are instantly captured and removed to the distal side of the nanopore) yields:

$$J = R_c c$$
$$R_c = \frac{2\pi D r^*}{1 - e^{-r^*/r_0}} \qquad \text{S7}$$

where

$$r^* = \frac{\mu q_{eff}}{\varepsilon D}$$
$$q_{eff} = \frac{\varepsilon d^2}{8l}\Delta V \qquad \text{S8}$$

In our system, d = 20-30 nm, l = 15 nm, ΔV= 30-80 mV, μ ≈ 10^{-9} –10^{-8} m^2/ s.V, and D ≈ 10^{-11} – 10^{-10} m^2/ s, so

$r^* \approx 10^{-2}$

Then

$$R_c \approx 2\pi D r^* \qquad \text{S9}$$

and

$$J = 2\pi D r^* c \qquad \text{S10}$$

S6- Nanopore measurements in the presence of hydrogels cross-linked to *trans* side of chip

We modified the SiN surface of the nanopore chip with 3-(Trimethoxy silyl) propyl methacrylate (Sigma-Aldrich) before the nanopore was formed, allowing the hydrogel to bond to the chip surface when curing. Following hydrogel curing, the nanopore was formed as described above, and following a regular control experiment, IgG was injected into the fluid cell.

We observed a significant increase in the event rate compared to unbonded hydrogel (200 Hz at 25 nM using the hydrogel-bonded nanopore compared to around 9-31 Hz at the same concentration using different hydrogel-backed /unbonded nanopores at - 50 mV), a significant increase in the average dwell times (event length) of detected protein (from hundreds of microseconds to milliseconds), and the dwell time as a function of voltage showed a strongly increasing trend compared to the unbonded hydrogel (Figure S4).

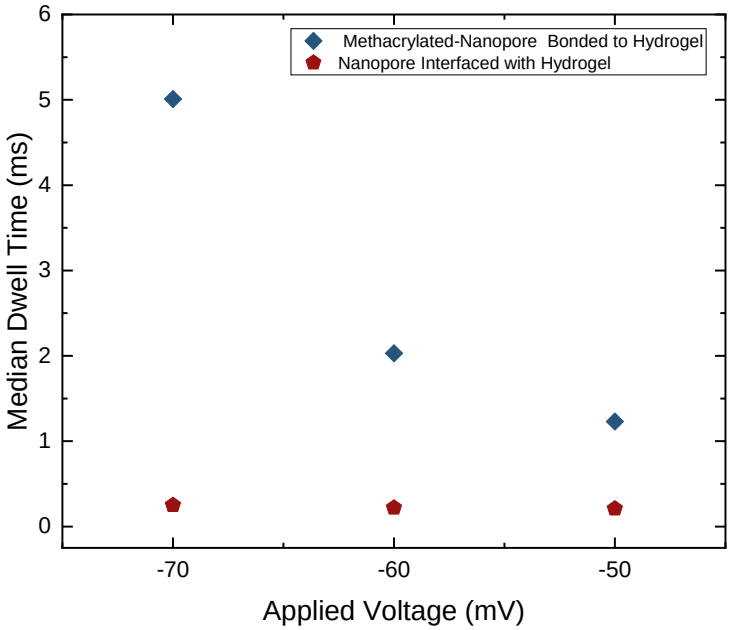

Figure S4. The median dwell times were obtained from data sets recorded for three voltages on nanopores with hydrogel bonded and unbonded to the *trans* side of the chip.

The increasing dwell time with increasing voltage for the bonded hydrogel suggests that protein may escape by diffusing against the electric field to escape from the pore on the *cis* side. Assuming that the hydrogel is a perfectly reflecting barrier, and the *cis* entrance is an absorbing barrier (corresponding to particle escape) the first passage time is given by:[4]

$$t = 2\left(\frac{l^2}{2D}\right)\left(\frac{kT}{qV}\right)^2\left\{e^{\frac{qV}{kT}} - 1 - \frac{qV}{kT}\right\}$$

where D is the protein diffusion constant, l is the pore length, k is Boltzmann's constant, T is the temperature, q is the protein charge, and V is the applied voltage.

On the other hand, if the particle escaped the nanopore on the trans side by going into the hydrogel or into the gap between the hydrogel and the nanopore chip, we may expect that the dwell time would decrease with increasing voltage. The large change in results following the bonding to the chip may indicate that the hydrogel-chip gap escape mechanism is being minimized. Variations in hydrogel-chip gaps may also explain how nanopores of similar diameter can show significantly different event rates, as seen in Figure 1.

In support of this hypothesis, we plotted the slope of frequency versus concentration for the data sets in Figure 1 versus the median dwell times of the same data (Figure S5) and found that increasing dwell times were strongly correlated with high nanopore sensitivity (higher event rate per concentration).

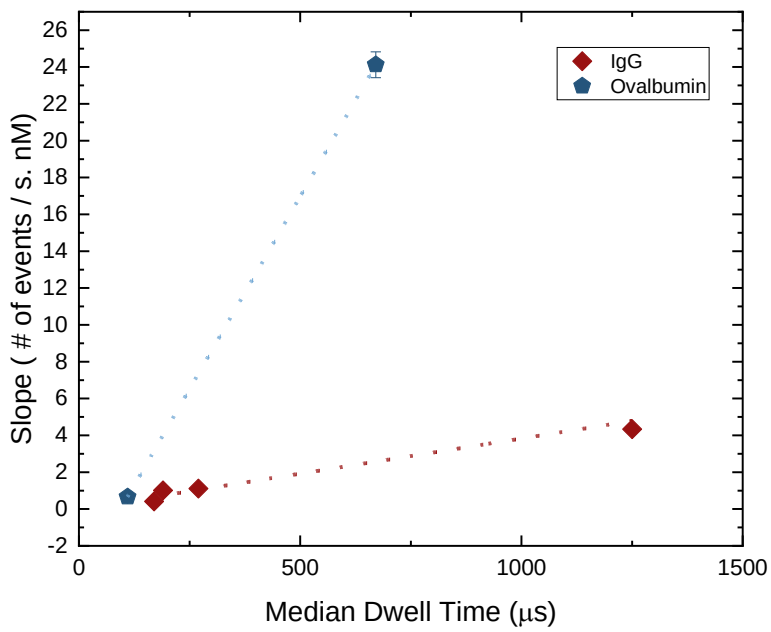

Figure S5. The slopes of the event frequency versus concentration lines from Figure 1 are plotted versus the median dwell times of the same data.

S7- Measurements of IgG using electrostatic focusing:

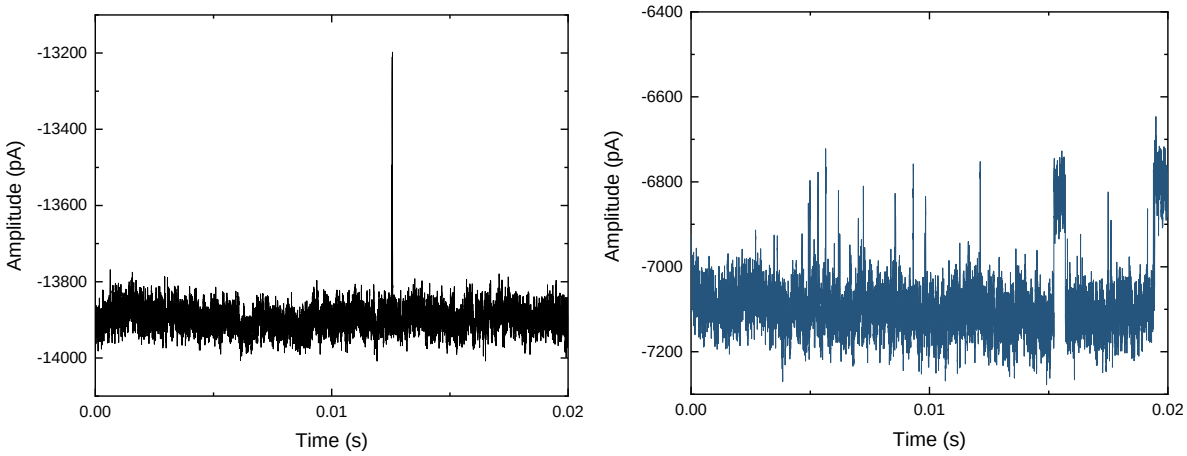

Figure S6: Left: Measurement of 10 pM IgG under symmetric 2 M/2 M KCl with a 29 nm diameter nanopore with hydrogel on *trans* side. Right: Measurement of 10 pM IgG with same nanopore but with 0.2 M KCL on the *cis* side.

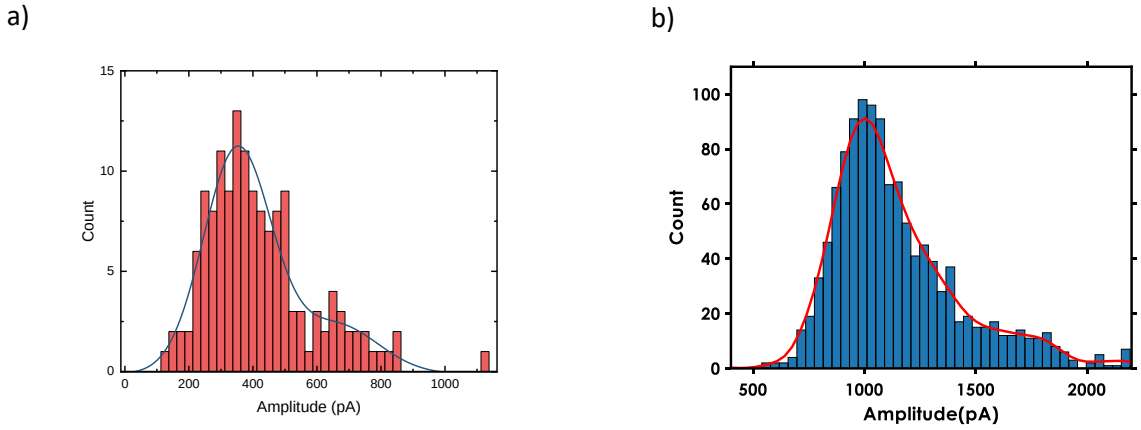

Figure S7. Amplitude histograms of the captured IgG events at (a) 100 fM under asymmetric salt gradient 0.2 M /2 M KCl and (b) 100 pM under symmetric salt gradient. Data from both panels obtained with -70 mV applied voltage.

S8- Estimation of protein excluded volume

The blockage current measured from a particle with the excluded volume Λ is derived from Maxwell's calculations on the resistivity of an insulating particle in the presence of an electromagnetic field. In the presence of an insulating particle inside an electrolyte-filled nanopore, the uniform electric field inside a cylindrical nanopore distorts slightly around the particle and changes the nanopore resistivity. The change in the resistivity of a nanopore depends both on the volume and orientation of the particle. For particles with volume much smaller than the volume of the cylindrical pore, Maxwell's expression simplifies to:[5,6]

$$\frac{\Delta R}{R} = \gamma \frac{\Lambda}{V} \qquad \text{S12}$$

where R is the pore resistance, ΔR is the change in pore resistance due to the presence of the particle, γ is the particle's electric shape factor (a function of the particle shape and orientation relative to the pore axis), and V is the pore volume.

For a sphere, γ is 3/2, and for ellipsoidal particles the extremes of γ are related to demagnetization factors:[6]

$$\gamma_{\parallel} = \frac{1}{1 - n_{\parallel}}$$
$$\gamma_{\perp} = \frac{1}{1 - n_{\perp}} \qquad \text{S13}$$
$$n_{\parallel} + 2n_{\perp} = 1$$

where $\gamma_{\parallel}$ and $n_{\parallel}$ are the electric shape and demagnetization factors when the electric field is oriented in the same direction of the axis of revolution of the spheroid, and $\gamma_{\perp}$ and $n_{\perp}$ are the electric shape and demagnetization factors for the perpendicular orientation.

Parallel and perpendicular demagnetization factors are determined by the geometry of the spheroid and are proportional to m, the ratio of diameter "a" to thickness "b" of a spheroid (m = a / b). In the case of oblate (m < 1) and prolate (m > 1) spheroids, demagnetization factors are calculated from Equation S14 and S15:[7]

For oblate with m < 1:

$$n_{\parallel} = \frac{1}{1 - m^2}\left[1 - \frac{m}{\sqrt{1 - m^2}} cos^{-1} m\right] \qquad \text{S14}$$

For prolate with m > 1:

$$n_{\perp} = \frac{1}{m^2 - 1}\left[\frac{m}{\sqrt{m^2 - 1}} cosh^{-1} m - 1\right] \qquad \text{S15}$$

However, Equation S12 is only valid in the limit of very small insulating particles in comparison with the diameter of the nanopore. In that case, the distortion of the electric field restricts just to the surrounding of the particle. For a bigger particle, the electric field deformation around the particle expands toward the nanopore wall and this effect increases the measured blockage current beyond the linear dependence on the particle volume. Extensive theoretical and experimental studies have been conducted to determine the measured blockage amplitude with respect to the ratio of a particle to a nanopore diameters,[8–10] and different correction coefficients were introduced into Equation S12 to account for the extra increase in nanopore resistance due to the presence of large particles. DeBlois and Bean[8] derived and tabulated values of the correction factor for large spherical particles with $\left(\frac{d_{particle}}{d_{pore}}\right)^3 > 0.1$, presented in Table S2:

Table S2. Correction factors derived by DeBlois and Bean (Reprinted with permission from DeBlois, R. W.; Bean, C. P. Counting and Sizing of Submicron Particles by the Resistive Pulse Technique. *Rev. Sci. Instrum.* **1970**, *41* (7), 909–916. Copyright 1970. American Institute of Physics)

$\left(\frac{d_{particle}}{d_{pore}}\right)^3$	S	$\left(\frac{d_{particle}}{d_{pore}}\right)^3$	S
0	1.0	0.5	2.31
0.1	1.14	0.6	2.99
0.2	1.32	0.7	4.15
0.3	1.55	0.8	6.50
0.4	1.87	0.9	13.7

Introducing this correction factor into Equation S12 to correct Maxwell's first order approximation, and further substitution of open nanopore current ($I = \frac{V_{applied\ voltage}}{R_{\ nanopore} + R_{access\ resistance}}$) with nanopore resistance R, and the blockage current ΔI with the change in the resistance ΔR yields Equation S16:

$$\Delta I = \frac{\Lambda V_A \gamma}{\rho\left(l_p + 0.8 d_{pore}\right)^2} S \left(\frac{d_{particle}}{d_{pore}}\right)^3 \qquad \text{S16}$$

where V_A is the applied voltage, γ is the protein's shape factor, ρ is the resistivity of the measurement buffer, and l_p is the nanopore length.

For a globular protein, we approximate γ = 3/2, and Equation S17 becomes:

$$\Delta I_{globular} = \frac{\frac{3}{2}\Lambda V_A}{\rho\left(l_p + 0.8 d_p\right)^2} S \left(\frac{d_{particle}}{d_{pore}}\right)^3 \qquad \text{S17}$$

For ellipsoidal proteins, the blockage current depends on the orientation of the protein within the nanopore. For oblate proteins, the blockage current is minimized when the protein axis is parallel to the nanopore axis and maximized when it is perpendicular.[5] Rewriting Equation S16 yields:

$$\Delta I_{ell_{min}} = \frac{\Lambda V_A \gamma_{\perp}}{\rho\left(l_p + 0.8d_p\right)^2} S\left(\frac{d_{particle}}{d_{pore}}\right)^3$$
$$\Delta I_{ell_{max}} = \frac{\Lambda V_A \gamma_{\parallel}}{\rho\left(l_p + 0.8d_p\right)^2} S\left(\frac{d_{particle}}{d_{pore}}\right)^3 \qquad \text{S18}$$

To calculate the protein volumes, we assume no prior knowledge about the size of the measured proteins, and consequently the ratio of protein to nanopore diameter for selection of an appropriate correction factor. We used the following iteration method to determine protein diameter and volumes. We start by the assumption that the protein diameter is much smaller than the nanopore diameter, and S = 1. Protein volume and hydrodynamic radius are calculated, and the ratio of protein to nanopore diameter is determined. This first approximation of the ratio of protein to nanopore diameter determines the next value of S read from Table S2. Then we use this new S to find the protein volume, hydrodynamic radius, and a new ratio of protein to nanopore diameter. This is repeated until the calculated ratio is the same as the ratio from the previous step. The protein volume and hydrodynamic radius is determined from this final value of S. For the proteins described in this work, this algorithm was convergent. Figure S8 summarizes this algorithm.

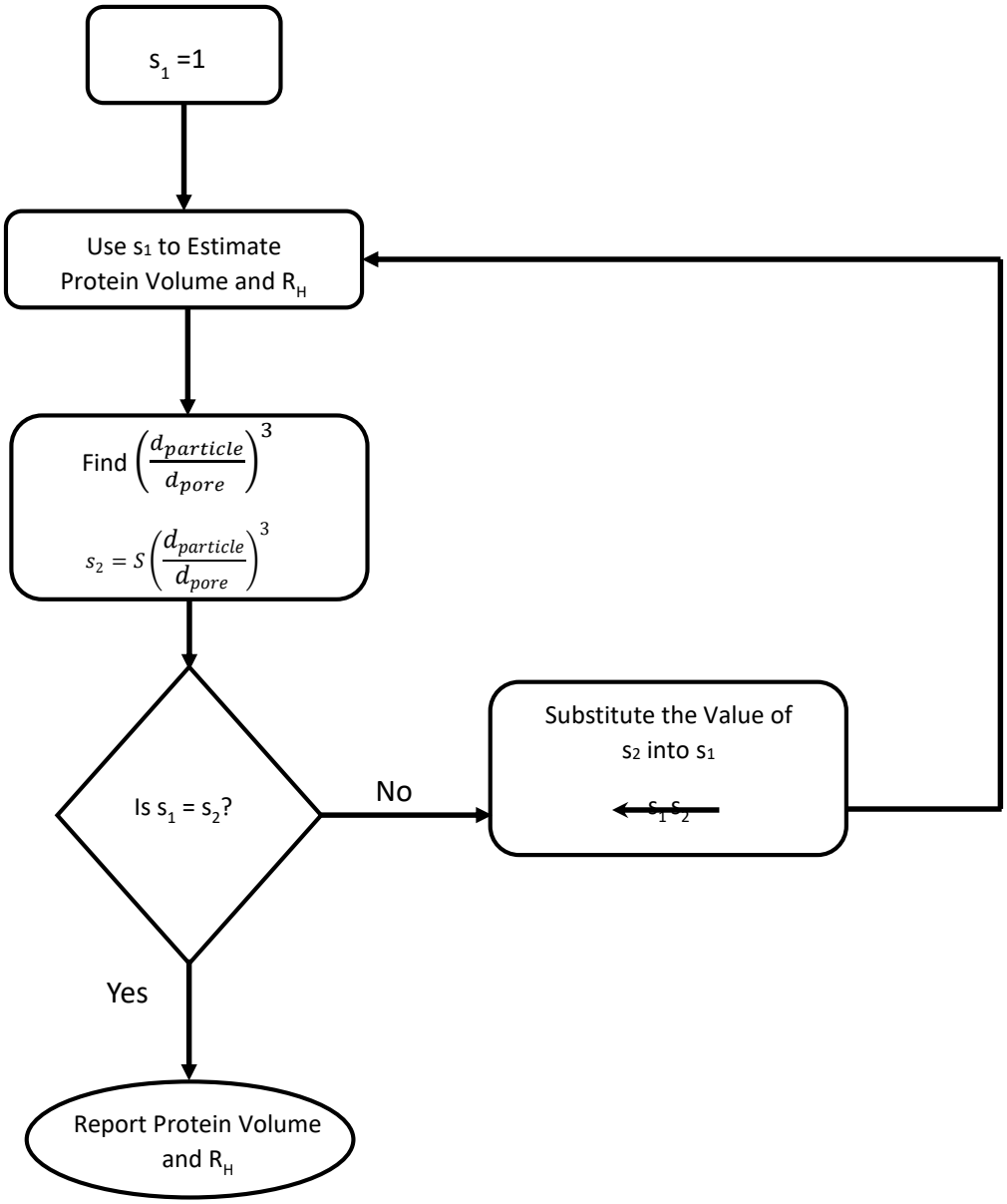

Figure S8. The iterative algorithm to find the protein volume and hydrodynamic radius R_H.

Protein excluded volume may also be estimated from its molecular weight:[11]

$$\Lambda = \frac{M}{N_A}(v1 + dv2) \qquad \text{S19}$$

where M is the protein's molecular weight, N_A is Avogadro's number, v_1 (0.74 cm^3/gr) and v_2 (1 cm^3/gr) are partial specific volumes of protein and water, and d (0.4) is the extent of protein hydration.

For a globular protein the hydrodynamic radius (R_H) is estimated by its radius, and for an oblate ellipsoid protein with semiaxes a, and b, the hydrodynamic radius is given by Equation S20:[12]

$$R_H = \frac{\sqrt{(b^2 - a^2)}}{\tan^{-1}\sqrt{\frac{(b^2 - a^2)}{a^2}}} \quad \text{S20}$$

For an oblate protein the volume is estimated by:

$$\Lambda = \frac{4}{24}\pi a b^2 \quad \text{S21}$$

a and b are related to each other as a = mb. m, the diameter to thickness of an ellipsoid, is calculated using Equation S14 and the ratio of $\gamma_{max}/\gamma_{min}$ is calculated using the Equation S13. Simultaneous solving of Equation S21 and S14 gives a and b, and hydrodynamic radius (R_H) is calculated using Equation S20.

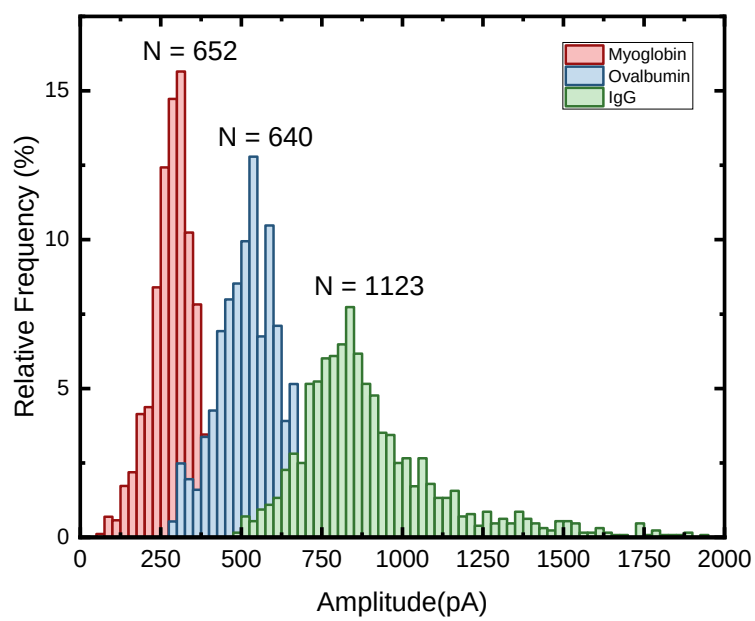

Figure S9: Measurement of myoglobin (18 kD), ovalbumin (44 kD), and IgG (160 kD) (concentrations 1-5 nM) using the same hydrogel-backed 18 nm diameter nanopore ("Pore A") for 7, 5, and 10 minutes, respectively. Each protein was measured separately with the solutions exchanged between measurements. -60 mV applied voltage. These distributions were analyzed using the algorithm described in Figure S8 to produce volume estimates shown in Table 1 of the manuscript, reproduced below (Table S3).

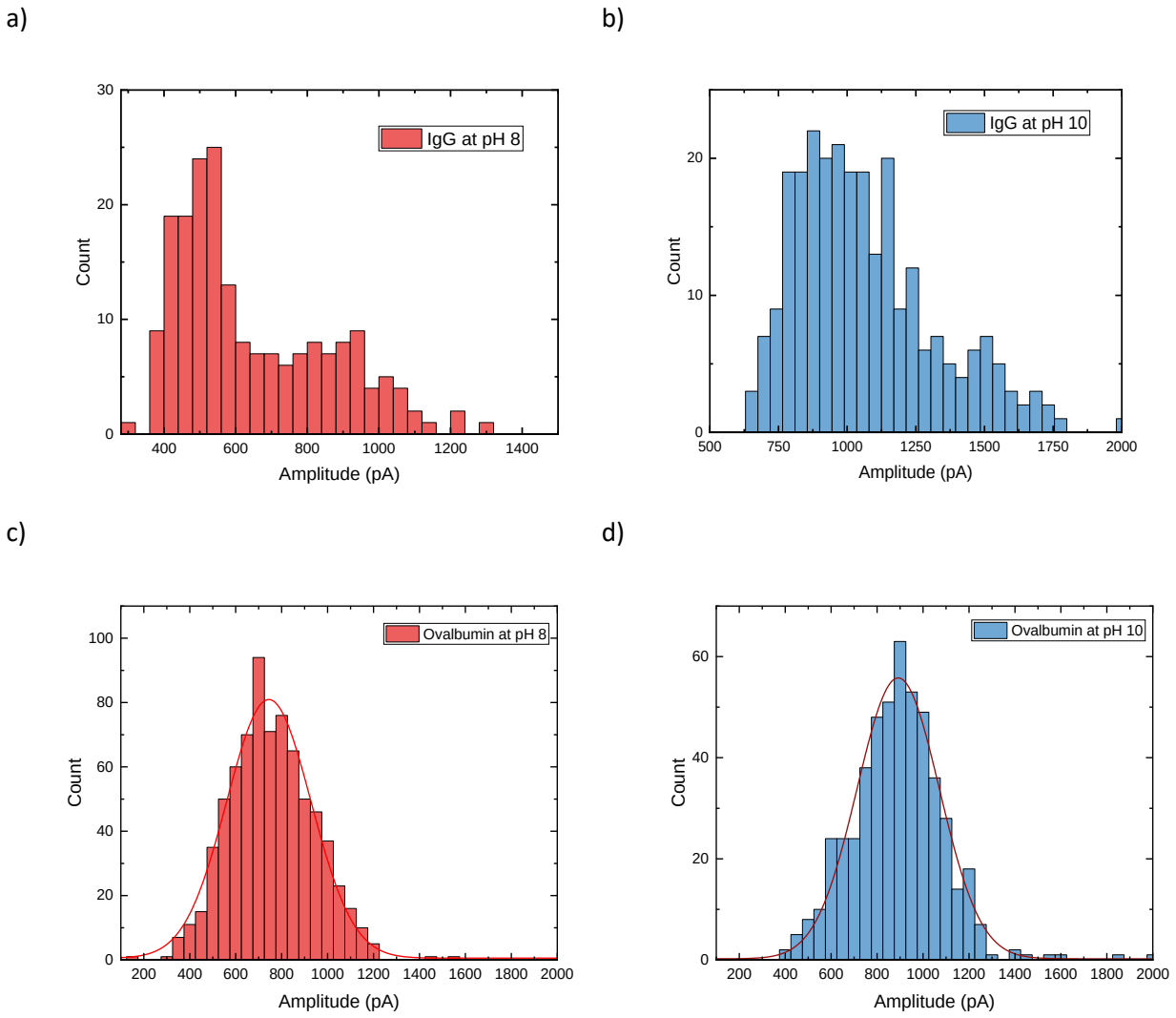

Figure S10: IgG measured at -70 mV applied voltage using a hydrogel-backed 21 nm diameter nanopore in 2 M KCl buffered to (a) pH 8 and (b) pH 10; Ovalbumin measured at -70 mV applied voltage using a hydrogel-backed 12 nm diameter nanopore in 2 M KCl buffered to (c) pH 8 and (d) pH 10. These distributions were analyzed using the algorithm described in Figure S8 to produce volume estimates shown in Table 1 of the manuscript, reproduced below (Table S3).

Table S3 (Reproduction of Table 1 from main manuscript)- Comparison of protein volumes measured using nanopores and dynamic light scattering for IgG, ovalbumin, and myoglobin

	Nanopore	Dynamic Light Scattering	
Protein	Excluded vol. (nm^3)	Hydrodynamic radius (nm)	Calculated vol. (nm^3)
IgG (pore A) IgG (pore B) IgG (pore B)	361 (pH 10) 376 (pH 10) 252 (pH 8)	5.5 (pH 7.4)[13]	258
Oval. (pore A) Oval. (pore C) Oval. (pore C)	235 (pH 10) 224 (pH 10) 197 (pH 8)	3.3 (pH 7.5)[14]	150
Myo. (pore A)	100 (pH 10)	2.4 (pH 7.4)[15,16]	58

S9- Capture rate of proteins with different hydrodynamic radius

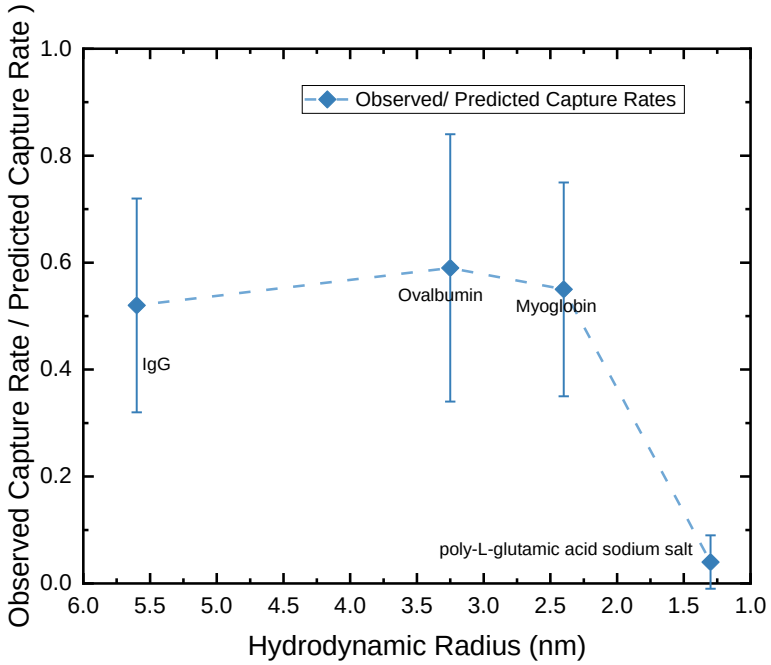

Figure S11. The ratio of observed to estimated capture rates for IgG (R_H =5.6 nm), ovalbumin (R_H =3.3 nm), and myoglobin (R_H =2.4 nm) at -50 mV applied voltage using hydrogel-backed 17-23 nm diameter nanopores. The ratio of observed to estimated capture rate for poly-L-glutamic sodium salt (R_H = 1.3 nm) was measured at -90 and -100 mV applied voltage using a hydrogel-backed 10 nm diameter nanopore.

References:

(1) Acharya, S.; Jiang, A.; Kuo, C.; Nazarian, R.; Li, K.; Ma, A.; Siegal, B.; Toh, C.; Schmidt, J. J. Improved Measurement of Proteins Using a Solid-State Nanopore Coupled with a Hydrogel. *ACS Sensors* **2020**, *5*, 370–376. https://doi.org/10.1021/acssensors.9b01928.

(2) Kowalczyk, S. W.; Grosberg, A. Y.; Rabin, Y.; Dekker, C. Modeling the Conductance and DNA Blockade of Solid-State Nanopores. *Nanotechnology* **2011**, *22* (31), 1–5. https://doi.org/10.1088/0957-4484/22/31/315101.

(3) Grosberg, A. Y.; Rabin, Y. DNA Capture into a Nanopore: Interplay of Diffusion and Electrohydrodynamics. *J. Chem. Phys.* **2010**, *133* (16). https://doi.org/10.1063/1.3495481.

(4) Howard, J. Mechanics of Motor Proteins and the Cytoskeleton; Sinauer Associates: Sunderland, MA, 2001; p 62.

(5) Yusko, E. C.; Bruhn, B. R.; Eggenberger, O. M.; Houghtaling, J.; Rollings, R. C.; Walsh, N. C.; Nandivada, S.; Pindrus, M.; Hall, A. R.; Sept, D.; Li, J.; Kalonia, D. S.; Mayer, M. Real-Time Shape Approximation and Fingerprinting of Single Proteins Using a Nanopore. *Nat. Nanotechnol.* **2017**, *12* (4), 360–367. https://doi.org/10.1038/nnano.2016.267.

(6) Golibersuch, D. C. Observation of Aspherical Particle Rotation in Poiseuille Flow via the Resistance Pulse Technique. II. Application to Fused Sphere " Dumbbells." *J. Appl. Phys.* **1973**, *44* (6), 2580–2584. https://doi.org/10.1063/1.1662616.

(7) Stoner, E. C. The Demagnetizing Factors for Ellipsoids. *London, Edinburgh, Dublin Philos. Mag. J. Sci.* **1945**, *36* (263), 803–821. https://doi.org/10.1080/14786444508521510.

(8) DeBlois, R. W.; Bean, C. P. Counting and Sizing of Submicron Particles by the Resistive Pulse Technique. *Rev. Sci. Instrum.* **1970**, *41* (7), 909–916. https://doi.org/10.1063/1.1684724.

(9) DeBlois, R. W.; Bean, C. P.; Wesley, R. K. A. Electrokinetic Measurements with Submicron Particles and Pores by the Resistive Pulse Technique. *J. Colloid Interface Sci.* **1977**, *61* (2), 323–335. https://doi.org/10.1016/0021-9797(77)90395-2.

(10) Gregg, E. C.; Steidley, K. D. Electrical Counting and Sizing of Mammalian Cells in Suspension. *Biophys. J.* **1965**, *5* (4), 393–405. https://doi.org/10.1016/S0006-3495(65)86724-8.

(11) Schneider, S. W.; Lärmer, J.; Henderson, R. M.; Oberleithner, H. Molecular Weights of Individual Proteins Correlate with Molecular Volumes Measured by Atomic Force Microscopy. *Pflugers Arch. Eur. J. Physiol.* **1998**, *435* (3), 362–367. https://doi.org/10.1007/s004240050524.

(12) He, L.; Niemeyer, B. A Novel Correlation for Protein Diffusion Coefficients Based on Molecular Weight and Radius of Gyration. *Biotechnol. Prog.* **2003**, *19* (2), 544–548. https://doi.org/10.1021/bp0256059.

(13) Karow, A. R.; Götzl, J.; Garidel, P. Resolving Power of Dynamic Light Scattering for Protein and Polystyrene Nanoparticles. *Pharm. Dev. Technol.* **2015**, *20* (1), 84–89. https://doi.org/10.3109/10837450.2014.910808.

(14) Plesa, C.; Kowalczyk, S. W.; Zinsmeester, R.; Grosberg, A. Y.; Rabin, Y.; Dekker, C. Fast Translocation of Proteins through Solid State Nanopores. *Nano Lett.* **2013**, *13* (2), 658–

663. https://doi.org/10.1021/nl3042678.

(15) Malvern Application Note-Measurement and Molecular Weight Estimation of Globins. *Malvern Instruments Worldw*. **2009**, 1–4.

(16) Lorber, B. Analytical Light Scattering Methods in Molecular and Structural Biology: Experimental Aspects and Results. **2018**, *ffhal-0166*, 1–41.